Ultrasound in Med. & Biol., Vol. 47, No. 3, pp. 386–397, 2021

0301-5629/$ - see front matter

https://doi.org/10.1016/j.ultrasmedbio.2020.10.008

● *Original Contribution*

ULTRASOUND IMAGING AS A DIAGNOSTIC TOOL TO ASSESS THE FUNCTIONAL STATUS OF MUSCLES AFTER A SPINAL CORD INJURY

JENNIFER MILLER,*,† HENRIK GOLLEE,*,† and MARIEL PURCELL†

* Centre for Rehabilitation Engineering, James Watt School of Engineering, University of Glasgow, Glasgow, United Kingdom; and † Queen Elizabeth National Spinal Injuries Unit, Queen Elizabeth University Hospital, Glasgow, United Kingdom

(*Received* 23 *July* 2020; *revised* 14 *October* 2020; *in final from* 17 *October* 2020)

Abstract—The aim of this study was to evaluate the use of ultrasound imaging (USI) as a diagnostic tool to assess muscle function after a spinal cord injury (SCI). Ultrasound videos of the gastrocnemius medialis muscle were recorded both at rest and during attempted maximum voluntary contraction (MVC) for fifteen participants with a SCI and fifteen able-bodied controls. Measurements were repeated at monthly intervals for participants in the SCI group during their inpatient stay. Differences in muscle echogenicity and thickness were detected between both able-bodied and SCI groups and subgroups of SCI participants, suggesting USI can detect and monitor changes in muscle structure which are characteristic of atrophy. Decreased muscle movement in the SCI groups was also detected during attempted MVC. The ability of USI to distinguish between different levels of function demonstrates the potential of USI as a quantitative tool to assess muscles. (E-mail: j.miller.6@research.gla.ac.uk)

Key Words: **Skeletal muscle, Spinal cord injury, Ultrasound imaging.**

INTRODUCTION

The spinal cord is part of the central nervous system and forms the main connection between the brain and the rest of the body, allowing communication by transmitting sensory and motor signals. When the spinal cord is injured, this exchange of information is disrupted, often leading to muscle paralysis and loss of sensation (Silva et al. 2014). Although the muscles are not directly affected by the injury, the lack of activation that follows results in structural changes within weeks, months or even years after the injury has occurred. These changes include a reduction in the size and number of muscle fibres, known as muscle atrophy. This is attributed either to denervation, where the motor neurons themselves are damaged, or disuse, where damage to the spinal cord blocks synaptic input from higher segments and results in a lack of muscle activation (Gordon and Mao 1994; Castro et al. 1999; Biering-Sprensen et al. 2009). In the spinal cord injury (SCI) population, muscles are also more susceptible to fatigue, which is thought to be caused by fibre-type transformation: A shift in fibre composition results in a higher proportion of fast-twitch fibres that are less resistant to fatigue (Gordon and Mao 1994; Burnham et al. 1997).

Currently, neuromuscular status in the SCI population is assessed with a physical examination known as a manual muscle test, in which a clinician grades a muscle's ability to generate a contraction (Kirshblum et al. 2011). The results from these tests can then be combined with the results of sensory tests to yield an overall grade on the American Spinal Injuries Association (ASIA) Impairment Scale. Electromyography can also be used to provide quantitative measurements of muscle activity. These tests provide valuable information; however, they are limited in their ability to differentiate between different muscles, assess deeper muscles, or detect very small muscle movements (Ellaway et al. 2011).

There is a need for more quantitative and sensitive assessment methods to describe the structural and functional changes in muscles after a SCI, to assess recovery and provide an accurate prognosis. Furthermore, improved assessment methods would facilitate the

Address correspondence to: Jennifer Miller, Research Mezzanine, Queen Elizabeth National Spinal Injuries Unit, Queen Elizabeth University Hospital, Glasgow, G51 4TF, UK. E-mail: j.miller.6@research.gla.ac.uk

implementation of appropriate rehabilitation strategies and allow the effectiveness of emerging technologies to be evaluated. Modalities such as magnetic resonance imaging (Gorgey and Dudley 2007) and dual-energy X-ray absorptiometry (Giangregorio and McCartney 2006) have been reported to provide measurements of the changes that occur in muscles as the result of atrophy; however, because of cost and accessibility, these techniques are limited to research and are not often used in a clinical setting. Measurements of bioelectrical impedance can also be used to monitor muscle mass; however, these results should be interpreted with caution as they are influenced by fluid retention (Nakanishi et al. 2019).

Over recent years, ultrasound imaging (USI) has emerged as an additional tool for the assessment of muscles. By allowing internal structures such as muscles to be visualised, descriptions of morphology including size, shape and structure can be obtained. Furthermore, the dynamic nature of USI allows muscle activity to be measured through changes in these parameters during contractions (Whittaker et al. 2007; Daniels and Dexter 2013).

Ultrasound imaging of skeletal muscles is well established, with several studies describing its ability to make accurate measurements of muscle size and establishing relationships between muscle activity and changes in architectural parameters (Narici et al. 1996; Hodges et al. 2003; Shi et al. 2007; Mayans et al. 2012; Lindberg et al. 2013). These changes in architectural parameters are often compared with measurements of torque obtained from a dynamometer (Ichinose et al. 2000; Reeves and Narici 2003; Maganaris et al. 2006; Chen et al. 2012). In this study, this is done to provide a comparative measurement of muscle function in the lower limb. In addition, recent technological advances allow USI to obtain these measurements with excellent resolution.

Since the work of Heckmatt et al. (1980), USI has also been widely used to screen for several neuromuscular abnormalities (Brockmann et al. 2007; Pillen et al. 2007, 2008; Grimm et al. 2015; Harding et al. 2016). Characteristics such as increased muscle echogenicity, that is, how bright or white the muscle appears on the ultrasound image, and reduced muscle thickness allow the use of USI to reliably detect muscle abnormalities such a muscular dystrophy and motor neuron disease. Various presentations of these key measurements allow differentiation between different disorders, particularly between myopathies and neuropathies (Pillen et al. 2008). Grimm et al. (2013) and Cartwright et al. (2013) also found that similar changes occurred in people who were hospitalised for a prolonged period. In these cases, the muscles were not directly affected by disease but were immobilised because of the illness.

Despite the wide range of studies indicating the use of USI as a diagnostic tool, to our knowledge the only work that has investigated its use for assessing muscles affected by SCI was Bjerkefors et al. (2015), which focused on the detection of muscle movement but did not investigate the morphology of the muscle.

The aim of this study was to evaluate the use of USI as a diagnostic tool to assess muscles after a SCI by recording ultrasound videos of muscles in both healthy and SCI populations and making measurements of muscle morphology. The hypothesis is that USI will be able to detect changes in muscle structure as a result of atrophy and differentiate between different levels of function.

METHODS

Participants

Fifteen participants with a SCI (9 male and 6 female, 55 ± 18 y [mean ± SD]) and 15 able-bodied participants (ABs) of the same sex and comparable age (54 ± 16 y [mean ± SD]), were recruited for this study. Written informed consent was given by all participants. Ethics approval was obtained from the Regional National Healthcare Research Ethics Committee, and the study was performed in accordance with the Declaration of Helsinki.

Participants with a SCI were inpatients at the Queen Elizabeth National Spinal Injuries Unit, Glasgow, who had an incomplete SCI affecting their lower limbs and were expected to remain inpatients for at least 3 months. Able-bodied participants were in self-reported good health with no known neuromuscular disorders. Participants in the SCI group completed monthly sessions until they were discharged, all completing at least three sessions except for one participant who withdrew from the study after only two sessions. Each of the ABs completed a single session. Demographic information for all participants in the study is provided in Table 1. It should be noted that although two participants presented as ASIA A on admission, all participants had an incomplete injury by the first session (*i.e.,* at least ASIA B).

Experimental procedures

Participants were seated on the chair of a dynamometer (Biodex, Shirley, NY, USA) with their right foot strapped to the attachment to record ankle torque, as illustrated in Figure 1. A linear ultrasound probe (LV7.5/60/128 Z-2), 59 mm in length with a 50 mm scanning depth, was connected to an ultrasound device (Echo Blaster 128, both Telemed, Vilnius, Lithuania) and was secured over the gastrocnemius medialis (GM) muscle

Table 1. Demographics of participants

SCI ID No.	Age (y)*	Sex	Injury level	ASIA score†	Time since injury (wk)‡	No. of sessions
1	63 [58]	M	C4	C	9	3
2	20 [24]	F	C4	C	9	3
3	23 [25]	F	T11	A	13	4
4	79 [77]	M	C4	C	4	2
5	49 [54]	F	C5	D	6	4
6	67 [58]	F	C7	A	12	6
7	48 [43]	F	C6	C	13	3
8	58 [57]	M	C4	C	8	5
9	53 [56]	M	C4	C	6	6
10	46 [47]	M	C4	C	8	7
11	35 [39]	F	C5	C	8	5
12	73 [74]	M	C2	D	10	5
13	71 [71]	M	T9	D	8	4
14	67 [67]	M	C2	C	11	4
15	67 [62]	M	T10	C	9	3
Summary	55 ± 18 [54 ± 16]	9 M 6 F	C4–T11	A: 2 C: 10 D: 3	9 ± 3	4 ± 1

SCI = spinal cord injury.
* Age of SCI participant [able-bodied control].
† ASIA score obtained on admission.
† Time since injury at assessment session 1.

using a custom-made bracket, with water-based ultrasound gel applied between the probe and the skin.

Ultrasound videos of the GM muscle and ankle torque were recorded while the muscle was at rest and during attempted maximum voluntary contractions (MVCs), where participants were instructed to contract their muscle as strongly as possible for approximately 10 s. Ultrasound videos were recorded using Echowave software (Telemed), and the output of the dynamometer was acquired on a data acquisition card (DAQCard 6036 E, National Instruments, Austin, TX, USA). The experiments were run using custom-written MATLAB scripts and Simulink models (R2014b, The MathWorks, Natick, MA, USA), and data were processed offline.

The GM was selected as ultrasound images of this muscle reveal clear parallel boundaries, allowing the use of software to track changes in muscle shape. This software, which is described in detail in the next section, has previously been reported to be successful in tracking changes in the shape of the GM (Darby et al. 2012).

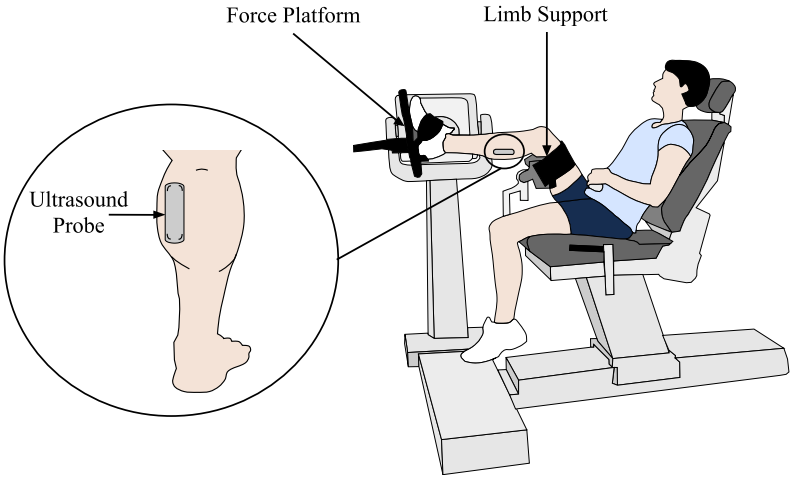

Fig. 1. Diagram of experimental setup depicting participant seated on chair of dynamometer with the ultrasound probe over the gastrocnemius muscle.

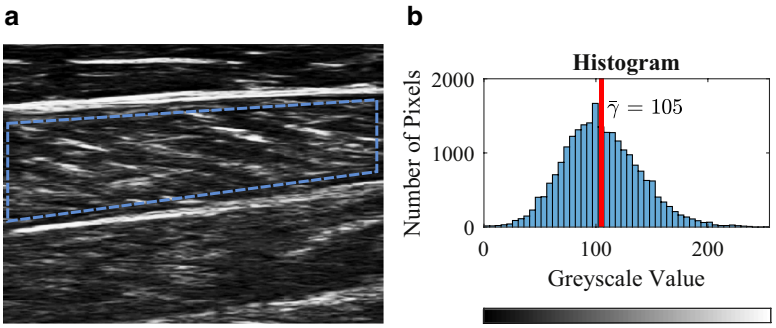

Fig. 2. (a) Ultrasound image of gastrocnemius muscle with selected region of interest. (b) Corresponding histogram of pixel gray-scale values; the *red line* represents the mean value ($\overline{\gamma}$).

Data analysis

Muscle echogenicity. Greyscale analysis quantitatively describes the echogenicity of the muscle for a single frame. A region of interest (ROI) was manually selected to include the largest possible area of the muscle but not the aponeuroses. Only pixels within this ROI were used for the greyscale analysis. Histograms allow the distribution of pixel grey-scale values to be evaluated, as illustrated in Figure 2. The mean ($\overline{\gamma}$) was also calculated to describe muscle echogenicity as a single representative value

$$\overline{\gamma} = \frac{\sum_{i=1}^{N} \gamma_i}{N} \quad (1)$$

where γ_i is the grey-scale value of the ith pixel, and N is the total number of pixels within the ROI.

Tracking of muscle shape. Measurements of muscle thickness and regional displacement were obtained using tracking software developed by Darby et al. (2012): A commonly used algorithm for shape detection, the active shape model (ASM), performs automatic segmentation by carrying out a probabilistic search for known shapes in new images to separate the upper and lower aponeuroses from the muscle tissue itself. The ASM is created by manually labelling frames with marker points on the boundaries of the muscle to create a point distribution model, which models variations in shape, and combining this with a Gaussian model of pixel intensity at each marker. The Hessian matrix, which describes local curvature using pixel intensity, is then used to select features that are tracked by the Lucas–Kanade–Tomasi (KLT) tracking algorithm. Features are tracked frame to frame by aligning the feature template with the new image. Regional movement is then quantified by a matrix of measurement probes placed across the image. The position of the probes is initialised based on the ASM segmentation on the first frame, and is then updated in each subsequent frame based on triangular interpolation of the KLT features. Figure 3 is a visual representation of each of these steps implemented in the tracking software. Figure 3a illustrates the automatic segmentation process used to calculate muscle thickness, while Figure 3b illustrates the matrix of measurement probes used to calculate displacement, numbered according to row and column.

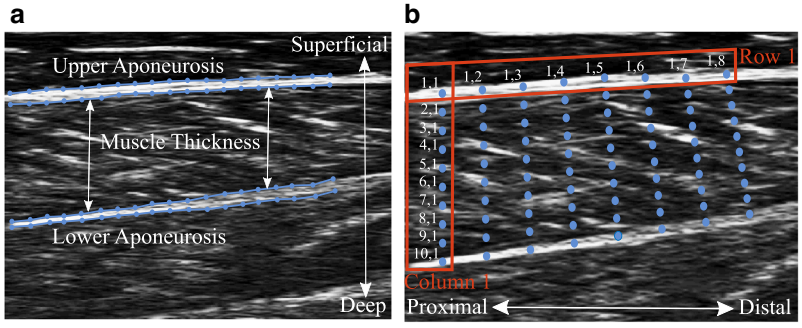

Fig. 3. Ultrasound image of the gastrocnemius muscle annotating the two main steps in the tracking software: (a) segmentation and (b) feature tracking.

Muscle thickness (Θ) is calculated based on the position of the markers along the muscle boundaries and is defined as the average distance between the upper and lower aponeuroses

$$\Theta = \frac{\sum_{i=1}^{M} \sqrt{\left(x_{(U,i)} - x_{(L,i)}\right)^2 + \left(y_{(U,i)} - y_{(L,i)}\right)^2}}{M} \quad (2)$$

where $\{x_{(U,i)} - y_{(U,i)}\}$ and $\{x_{(L,i)} - y_{(L,i)}\}$ are the x and y coordinates of the ith marker on the upper (subscript U) and lower (subscript L) aponeurosis, respectively, and M is the number of markers placed along each muscle boundary.

Muscle deformation (δ) is the change in muscle thickness, $\Delta\Theta = \Theta - \Theta_0$, as a percentage of the resting thickness (Θ_0):

$$\delta = \frac{\Delta\Theta}{\Theta_0} \times 100\% \quad (3)$$

Muscle displacement is the regional movement within the muscle and is defined as the summation of the changes in measurement probe position (Δp) between adjacent frames,

$$\Delta p_{mn}(f) = \sum \sqrt{(x_{mn}(f) - x_{mn}(f-1))^2 + (y_{mn}(f) - y_{mn}(f-1))^2} \quad (4)$$

where Δp_{mn} is the displacement of a measurement probe in row m and column n between frame number f and the previous frame.

The distance a measurement probe has travelled over several frames can also be used to calculate the average speed, v, of a muscle contraction during that period,

$$v_{mn} = \frac{\sum_{f=F_s}^{Fe} \Delta p_{mn}(f)}{t(F_e) - t(F_s)} \quad (5)$$

where v_{mn} is the average speed of a measurement probe in row m and column n, and $t(F_s)$ and $t(F_e)$ are the times corresponding to the frame at the start (F_s) and end (F_e) of the period, respectively.

In this study, the speed of muscle contraction was calculated during the first 2.5 s of an attempted MVC ($t(F_e) - t(F_s) = 2.5$ s). This time frame was chosen because it was found to be sufficient for participants to reach their maximum level of torque, allowing speed to be calculated for the initial phase of the contraction without taking into account the participant's attempt to sustain it.

Statistics

The Statistics Toolbox in MATLAB (R2019a, The MathWorks) was used for all statistical analysis. For all measures, normality was assessed using the Shapiro-Wilk test. A one-way analysis of variance was performed on data that were found to be normally distributed to determine whether or not different groups shared a common mean. In cases in which data were not normally distributed, the Kruskal–Wallis test was used instead. A p value <0.05 was considered to indicate a statistically significant difference.

Cohen's d effect size (Sawilowsky et al. 2011) was also calculated as an alternative measurement of the difference between two groups,

$$d = \frac{\bar{x}_1 - \bar{x}_2}{\sigma} \quad (6)$$

where $\bar{x}$ is the group mean, and σ is the standard deviation of the data.

Grouping of participants

For comparisons between the AB and SCI groups, measurements from all AB participants and all participants with SCIs for each session are included. To determine if USI could differentiate between different groups of SCI participants, the SCI group was further divided into subgroups on the basis of the following criteria:

1. Time post-injury: Participants with a SCI were divided into groups based on the time since their injury occurred. Based on the range of data collected, the three periods used were 0–3, 3–6 and 6–9 mo post-injury.
2. Torque level: Participants with a SCI were divided into groups based on the amount of torque they were able to produce during an attempted MVC. Based on the range of data collected and the torque values produced by the able-bodied controls (which were generally in the range of 20–60 N·m), 0–10 N·m was considered low-level torque, 10–20 N·m was considered medium-level torque and >20 N·m was considered a high level of torque.

There was a large variation in the time since injury at session 1 and the number of sessions completed by each SCI participant. There is also variation in the severity of the injury and the amount of recovery, meaning that some participants had improved torque levels, some had low-level torque throughout and some were able to produce high levels of torque during the first session. As a result, the different SCI groups do not contain the same number of measurements.

RESULTS

Muscle echogenicity

In Figure 4 are histograms of the greyscale values for all pixels, for time post-injury (Fig. 4a) and torque-level (Fig. 4b). In Figure 4a, SCI participants 0–3 mo post-injury exhibited a small shift to higher greyscale

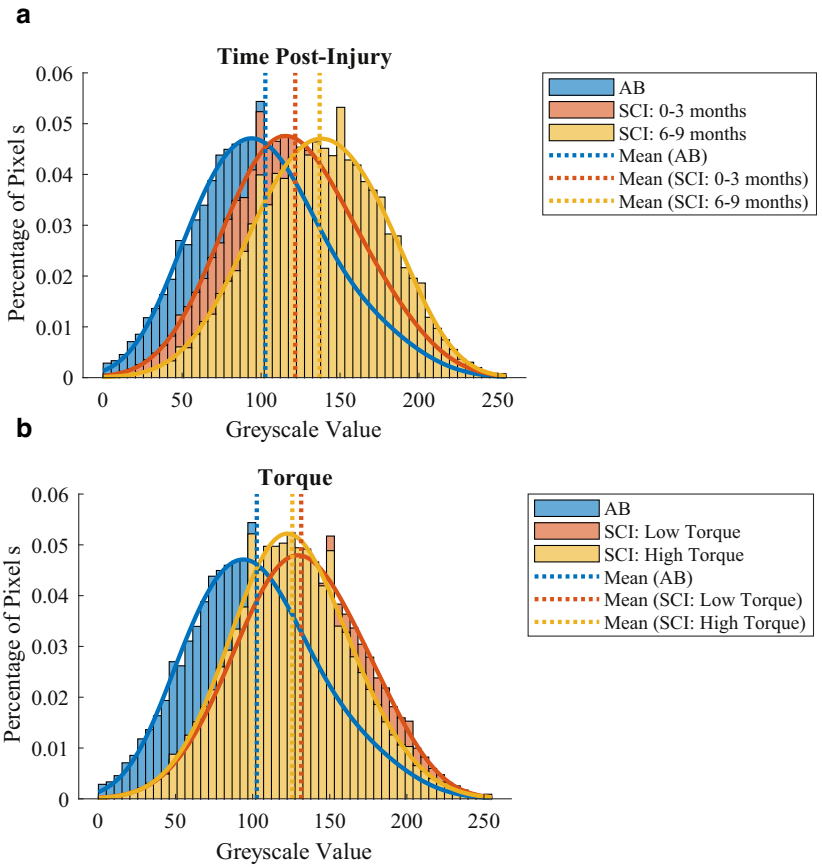

Fig. 4. Histograms of the greyscale values for AB participants and different groups of SCI participants. AB = able-bodied participants; SCI = participants with spinal cord injury.

values compared with able-bodied participants, whereas those 6−9 mo post-injury exhibited a larger shift to higher greyscale values, indicating the muscle ROI appears brighter. In contrast, there appears to be no difference between SCI participants with different torque levels, with histograms of SCI participants with low and high torque in Figure 4b showing a similar shift to higher greyscale values compared with the AB group.

The boxplots in Figure 5 confirm an increase in the mean gray-scale values for SCI participants compared

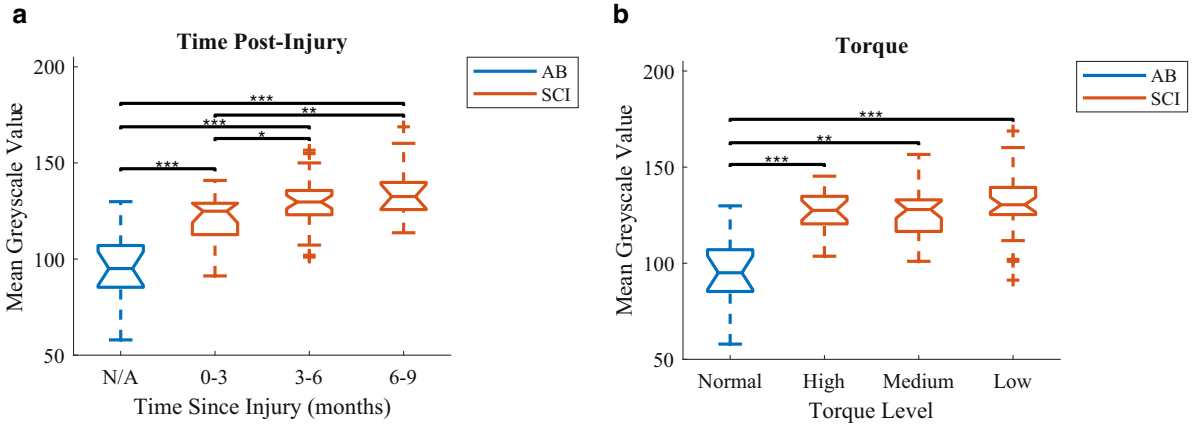

Fig. 5. Boxplots of the mean greyscale values of pixels for AB participants and different groups of SCI participants. *$p < 0.05$. **$p < 0.01$. ***$p < 0.001$. AB = able-bodied participants; SCI = participants with spinal cord injury.

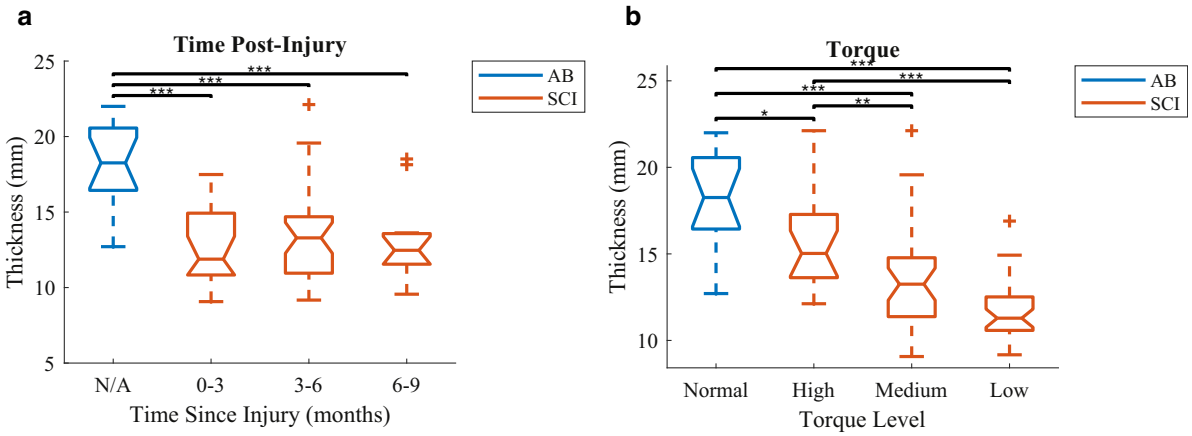

Fig. 6. Boxplots of the resting muscle thickness for AB participants and different groups of SCI participants. *$p < 0.05$, **$p < 0.01$. ***$p < 0.001$. AB = able-bodied participants; SCI = participants with spinal cord injury.

with able-bodied participants, with the AB group found to be statistically significantly different from all SCI groups. The difference in gray-scale values increases with time post-injury (see Fig. 5a). There is a statistically significant difference between SCI participants at 0−3 mo and SCI participants at 6−9 mo. The effect size between these two groups was found to be large ($d = 0.95$). There was also a statistically significant difference between SCI at 0−3 mo and SCI at 3−6 mo; however, only a medium effect size was calculated ($d = 0.65$). The results in Figure 5b illustrate that torque level does not appear to affect muscle echogenicity in SCI, with no statistically significant differences between SCI groups of different levels.

Muscle thickness

Figure 6 illustrates that the muscle was thinner for all SCI groups compared with the AB group, with each SCI group exhibiting a statistically significant difference from the AB group. Figure 6a indicates that there are no significant differences between different times post-injury within the SCI group; however, muscle thickness does appear to decrease with torque level (Fig. 6b). For SCI, low and high torque levels were found to differ significantly, which is associated with a very large effect size ($d = 1.39$). There is also a significant difference and a large effect size ($d = 1.01$) between medium and high torque levels in SCI. The difference between low and medium torque levels in SCI did not reach statistical significance, but had a medium effect size ($d = 0.65$). The p value and effect size for all measurements of the muscle at rest are given in Table 2.

Muscle behaviour during attempted MVC

In Figure 7 each of the main outcome measures is plotted over time for one AB participant and the age- and sex-matched SCI participant during an attempted MVC. Figure 7a illustrates the torque produced; Figure 7b, the

Table 2. p Values and Cohen's d effect size for measurements of the muscle at rest (mean greyscale and muscle thickness).

	Mean grey scale		Resting thickness	
	p Value	Effect size	p Value	Effect size
Time post-injury				
AB and 0−3 mo	1.75×10^{-4}	1.20	6.99×10^{-6}	1.38
AB and 3−6 mo	2.21	1.51	1.36×10^{-4}	1.25
AB and 6−9 mo	1.05×10^{-5}	1.46	7.59×10^{-4}	1.29
0−3 and 3−6 mo	0.03	0.65	0.59	0.26
0−3 and 6−9 mo	0.01	0.95	0.55	0.17
3−6 and 6−9 mo	0.29	0.42	0.70	0.10
Torque level				
AB and low	1.56×10^{-7}	1.44	4.70×10^{-7}	1.70
AB and medium	0.001	1.21	1.04×10^{-4}	1.40
AB and high	3.75×10^{-6}	1.39	0.03	0.76
Low and medium	0.03	0.65	0.07	0.65
Low and high	0.01	0.95	9.92×10^{-7}	1.39
Medium and high	0.29	0.42	0.01	1.01

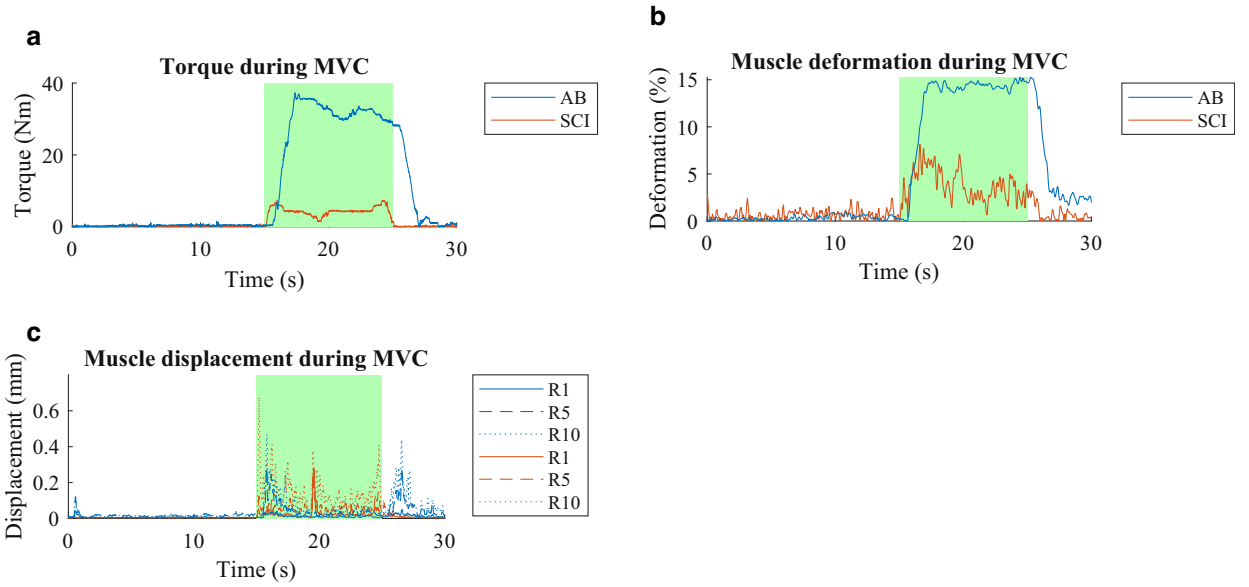

Fig. 7. Outcome measures plotted over time for a single AB participant and the age- and sex-matched SCI participant during attempted MVC. The green area represents the time during which participants were instructed to attempt the MVC ($t = 15–25$ s). AB = able-bodied participants; SCI = participants with spinal cord injury; MVC = maximum voluntary contraction.

deformation of the muscle; and Figure 7c, the displacement of the muscle at rows 1, 5 and 10 (cf. Fig. 3).

Muscle deformation during attempted MVC appears to be slightly lower for SCI participants than for AB participants, as illustrated in Figure 8. However, there are no significant differences between AB and SCI groups or between different SCI groups, and only small to medium effect sizes are observed.

A reduction in muscle displacement with decreasing torque level is seen in Figure 9a. There are significant differences between all torque levels within the SCI group for all positions of the muscle except row 1. All positions of the muscle also exhibit a significant difference between the AB group and SCI group with low torque. At row 10 and columns 4 and 8, there is also a significant increase between the AB group and SCI group with high torque.

A similar decrease with torque is also seen for the speed at which the muscle contracted during an attempted MVC (see Fig. 9b). There are significant differences between all torque levels in the SCI group for all muscle positions except row 1, where there is no significant difference between high and medium torque levels.

There are also significant differences between AB and all SCI groups in the superficial to deep direction (all rows), while in the proximal to distal direction, significant differences were seen only between low and medium torque (columns 1 and 4) or for low torque only (column 8).

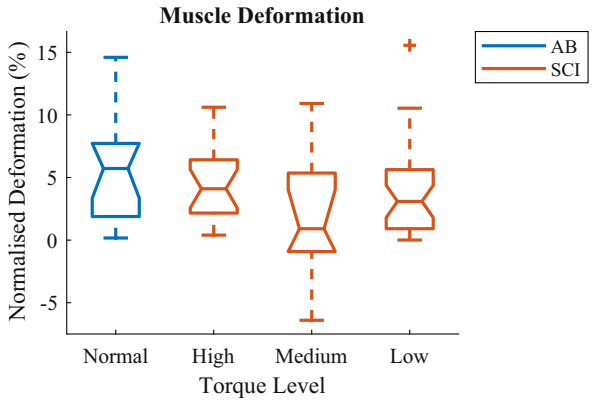

Fig. 8. Boxplots of maximum muscle deformation (δ) during attempted MVC for able-bodied participants and different groups of spinal cord injury participants. AB = able-bodied participants; SCI = participants with spinal cord injury; MVC = maximum voluntary contraction.

DISCUSSION

The aim of this study was to evaluate the use of USI as a diagnostic tool for assessing muscles affected by a SCI. Ultrasound videos of the GM in both able-bodied and SCI populations were recorded. Measurements of muscle echogenicity, resting thickness and muscle movement were made to assess how well USI can detect changes in muscle structure as a result of atrophy and how this relates to muscle function.

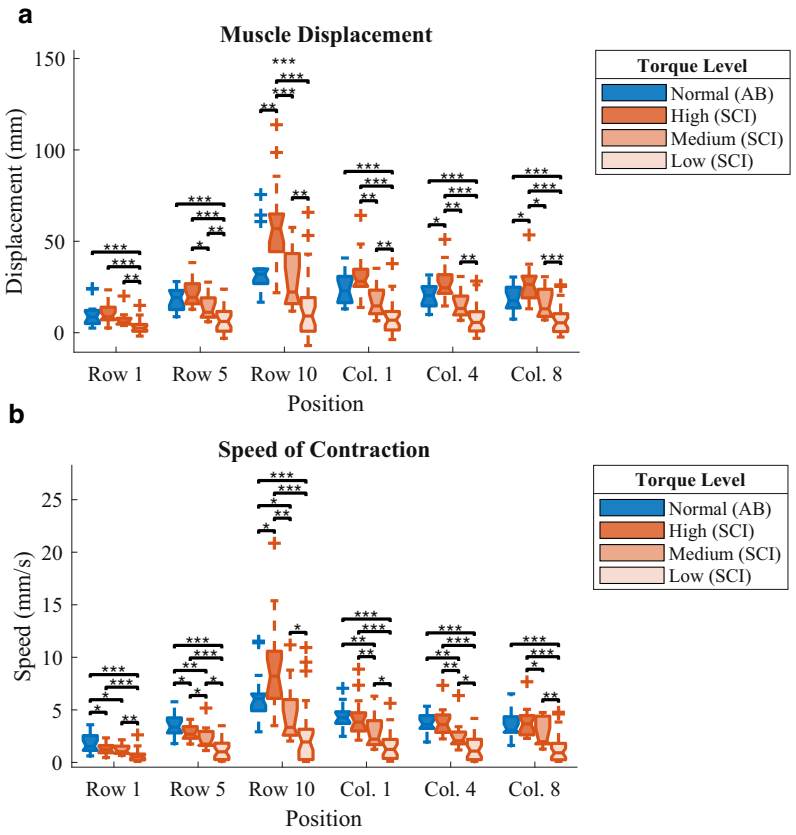

Fig. 9. Boxplots of muscle displacement measurements at different positions during attempted MVC for AB participants and different groups of SCI participants. *$p < 0.05$. **$p > 0.01$. ***$p > 0.001$). See Figure 3 for the row/column locations. AB = able-bodied participants; SCI = participants with spinal cord injury; MVC = maximum voluntary contraction.

The increase in the greyscale values of pixels indicates an increase in muscle echogenicity and agrees with the structural changes that occur in muscles as a result of atrophy. Muscles normally appear dark in ultrasound images as most of the sound waves emitted are absorbed by the tissue. In contrast, the connective tissue that surrounds both the muscle itself (epimysium) and the fascicles within the muscle (perimysium) have a different acoustic impedance and cause many of the sound waves to be reflected back to the ultrasound transducer as echoes. This results in the characteristic bright boundaries and striated appearance, which allow muscles to be easily identified. A muscle that appears brighter is generally an indication that there are a larger number of reflective surfaces (Pillen et al. 2008). One possible explanation for this increase in echogenicity in SCI is that as the muscle atrophies, the size and number of muscle fibres decrease, leading to a higher proportion of connective tissue, and fat infiltration occurs, both of which lead to an increased number of reflective surfaces.

It should also be considered that other factors such as increased subcutaneous tissue and oedema could contribute to the increase in greyscale values, as this would also cause an increase in reflective surfaces. The effects of this have been reduced as far as possible by considering only the pixels within a manually selected ROI that contains muscle tissue alone.

Whatever the exact mechanism, participants with a SCI exhibited an increase in the greyscale values of muscles. USI was able to detect statistically significant differences both between the AB group and SCI groups and between SCI groups at different times post-injury, suggesting that USI not only can detect muscle atrophy, but can also monitor its progression. As there is no statistically significant difference between SCI groups with different torque levels, it appears that this is not a factor that affects muscle echogenicity. This is in agreement with the findings of Gordon and Mao (1994), who suggested that muscle atrophy was not necessarily correlated with muscle activity, but appeared to be more affected by load bearing; that is, the GM muscle may be able to produce relatively high levels of torque but it will not be loaded if the other muscles in the legs do not support standing or walking. As all SCI participants in this study were

wheelchair users, this would explain why there is not a significant difference between different torque levels. Muscle shortening is also thought to be a factor that contributes to muscle atrophy (Baker and Matsumoto 1988; Pierotti et al. 1991), hence the presence of contractures could also explain differences in the amount of muscle atrophy. In contrast, it has been suggested that muscle spasticity may actually reduce the effects of disuse atrophy by maintaining muscle contractions (Cha et al. 2019). There are therefore several factors contributing to the amount of muscle atrophy besides the amount of torque the muscle is able to produce.

The reduction in resting muscle thickness seen between the able-bodied and SCI groups is also characteristic of muscle atrophy. As the number and size of muscle fibres decrease, it follows that the overall thickness of the muscle would also decrease. Again, USI was able to detect statistically significant differences between the AB and SCI groups and between different SCI groups. Conversely to the greyscale results, time since injury appeared to have no effect on muscle thickness, with no significant differences between the different groups. On the other hand, there were significant differences between low and high levels of torque, suggesting that measurements of muscle thickness are more representative of the functional status of the muscle. There is a statistically significant difference between medium and high torque but not between low and medium torque, and medium to high torque also has a larger effect size. This suggests that measurements of muscle thickness may be more sensitive to differences in torque levels above a certain threshold, possibly because of the infiltration of fat preserving some muscle bulk.

Overall, the combination of these measurements, muscle echogenicity and resting thickness, provides accurate information on the level of muscle atrophy. These changes in muscle structure could provide valuable information when assessing muscle function, implementing a rehabilitation strategy and assessing its effectiveness.

Ultrasound imaging also detected differences in muscle behaviour during attempted MVC; however, movement at the regional level appears to be much more useful than movement of the muscle as a whole. Muscle deformation, a measure of the thickness change of the entire muscle, did not statistically significantly differ between AB and SCI or different torque levels. This could be explained by surrounding muscles' compression of the GM muscle, resulting in the change in muscle thickness being measured not accurately representing the level of activation. This theory is further reinforced by the negative change in muscle thickness seen for some participants.

Muscle displacement, on the other hand, decreases with torque level, differing significantly between all SCI groups. This is to be expected as muscles more affected by paralysis will move less. This is seen consistently across all positions of the muscle except row 1. In general, muscle displacement is larger at deeper regions of the muscle compared with superficial areas. This would explain why less significant differences are seen at row 1 where there is less movement. Muscle movement in the proximal to distal direction appears to be more uniform.

Muscle displacement in the AB group appears to be similar to that of SCI groups with medium and high torque levels and, at some positions (row 10, column 4 and column 8), is even shown to be significantly less than that of the SCI group with high torque. Although this may seem counterintuitive, SCI participants whose muscles are more affected by fatigue may find it more difficult to maintain the contraction at a high torque level and, as a result, will move more during this phase of the contraction than an AB participant producing the same level of torque. As displacement is the summation of movement between frames, this would result in a higher measurement for SCI participants. This effect is seen most at row 10, where most movement occurs; therefore, the location of the measurement on the muscle should be taken into consideration when using USI as a tool for quantifying muscle movement.

Finally, the speed of muscle contraction during the first 2.5 s of an attempted MVC was found to be slower for SCI participants compared with able-bodied participants. This differs from previous studies (Burnham et al. 1997; Biering-Sprensen et al. 2009) that suggest muscle contractility increases as a result of a fibre-type transformation. It is generally accepted that after a SCI, there is a shift in fibre composition resulting in a higher proportion of fast-twitch type IIx fibres; however, there is variation between the different muscles being examined and the time post-injury when this fibre transformation is seen. It is thought that the fibre transformation may not begin until months after the SCI has occurred and could take years to reach a steady state. It is therefore possible that our measurements were made too soon after injury to observe these effects in participants in this study. In addition, the overall effect of this change in fibre composition on the contractile properties of the muscle in terms of speed of contraction is still not fully understood (Biering-Sprensen et al. 2009). Moreover, as these studies obtain their results from muscle biopsies, it could be that other factors such as muscle stiffness and delayed reaction times contributed to the lower speed of contraction seen here.

Overall, the ability of USI to consistently detect differences in muscle behaviour during an attempted MVC indicates its potential to quantitatively assess muscle movement and track how this changes during recovery.

CONCLUSIONS

This study found that USI is able to detect an increase in muscle echogenicity and a decrease in resting muscle thickness between able-bodied and SCI groups as well as between different SCI groups, indicating that it has potential as a diagnostic tool for monitoring changes in muscle structure caused by atrophy after a spinal cord injury. USI was also able to detect differences in regional movement during attempted MVCs. The ability of USI to differentiate between different levels of function means that it could also be used for quantitative assessment of muscles. The differences in the speed of muscle contraction illustrate the ability of USI to provide information on the contractile properties of the muscle, all of which could be useful when implementing rehabilitation techniques. In summary, USI was able to provide unique insight into the structural changes that occur in muscles after a SCI and has great potential as an additional tool for obtaining supplementary information for assessing muscle function in neuromuscular disease.

Acknowledgments—The authors thank I. Loram for his advice on analysing the ultrasound recordings. J.M. was supported by an EPSRC DTA scholarship [award number: EP/M508056/1].

Conflict of interest disclosure—The authors declare no conflict of interest.

REFERENCES

Baker JH, Matsumoto DE. Adaptation of skeletal muscle to immobilization in a shortened position. Muscle Nerve 1988;11:231–244.
Biering-Sprensen B, Kristensen IB, Kjaer M, Biering-Sprensen F. Muscle after spinal cord injury. Muscle Nerve 2009;40:499–519.
Bjerkefors A, Squair JW, Malik R, Lam T, Chen Z, Carpenter MG. Diagnostic accuracy of common clinical tests for assessing abdominal muscle function after motor-complete spinal cord injury above T6. Spinal Cord 2015;53:114–119.
Brockmann K, Becker P, Schreiber G, Neubert K, Brunner E, Bonneman C. Sensitivity and specificity of qualitative muscle ultrasound in assessment of suspected neuromuscular disease in childhood. Neuromuscul Disord 2007;17:517–523.
Burnham R, Martin T, Stein R, MacLean I, Steadward R. Skeletal muscle fibre type transformation following spinal cord injury. Spinal Cord 1997;35:86–91.
Cartwright MS, Kwayisi G, Griffin LP, Sarwal A, Walker FO, Harris JM, Berry MJ, Chahal PS, Morris PE. Quantitative neuromuscular ultrasound in the intensive care unit. Muscle Nerve 2013;47:255–259.
Castro MJ, Apple DF, Hillegass EA, Dudley GA. Influence of complete spinal cord injury on skeletal muscle cross-sectional area within the first 6 months of injury. Eur J Appl Physiol Occup Physiol 1999;80:373–378.
Cha S, Yun J, Myong Y, Shin H. Spasticity and preservation of skeletal muscle mass in people with spinal cord injury. Spinal Cord 2019;57:317–323.
Chen X, Zheng YP, Guo JY, Zhu Z, Chan SC, Zhang Z. Sonomyographic responses during voluntary isometric ramp contraction of the human rectus femoris muscle. Eur J Appl Physiol 2012;112:2603–2614.
Daniels JM, Dexter WW. Basics of musculoskeletal ultrasound. New York: Springer; 2013.
Darby J, Hodson-Tole EF, Costen N, Loram ID. Automated regional analysis of B-mode ultrasound images of skeletal muscle movement. J Appl Physiol 2012;112:313–327.
Ellaway PH, Kuppuswamy A, Blasubramaniam AV, Maksimovic R, Gall A, Craggs MD. Development of quantitative and sensitive assessments of physiological and functional outcome during recovery from spinal cord injury: A clinical initiative. Brain Res Bull 2011;84:343–357.
Giangregorio L, McCartney N. Bone loss and muscle atrophy in spinal cord injury: Epidemiology, fracture prediction, rehabilitation strategies. J Spinal Cord Med 2006;29:489–500.
Gordon T, Mao J. Muscle atrophy and procedures for training after spinal cord injury. Phys Ther 1994;74:56–67.
Gorgey AS, Dudley GA. Skeletal muscle atrophy and increased intramuscular fat after incomplete spinal cord injury. Spinal Cord 2007;45:304–309.
Grimm A, Teschner U, Porzelius C, Ludewig K, Zielske J, Witte OW, Brunkhorst FM, Axer H. Muscle ultrasound for early assessment of critical illness neuromyopathy in severe sepsis. Crit Care 2013;17:R227.
Grimm A, Prell T, Decard BF, Schumacher U, Witte OW, Axer H. Muscle ultrasonography as an additional diagnostic tool for the diagnosis of amyotrophic lateral sclerosis. Clin Neurophysiol 2015;126:820–827.
Harding PJ, Loram ID, Combes N, Hodson-Tole EF. Ultrasound-based detection of fasciculations in healthy and diseased muscles. IEEE Trans Biomed Eng 2016;63:512–518.
Heckmatt JZ, Dubowitz V, Leeman S. Detection of pathological change in dystrophic muscle with B-scan ultrasound imaging. Lancet 1980;315:1389–1390.
Hodges PW, Pengel LH, Herbert RD, Gandevia SC. Measurement of muscle contraction with ultrasound imaging. Muscle Nerve 2003;27:682–692.
Ichinose Y, Kawakami Y, Ito M, Kanehisa H, Fukunaga TF. In vivo estimation of contraction velocity of human vastus lateralis muscle during “isokinetic” action. J Appl Physiol 2000;88:851–856.
Kirshblum SC, Burns SP, Biering-Sprensen F, Donovan W, Graves DE, Jha A, Johansen M, Jones L, Krassioukov A, Mulcahey MJ, Schmidt-Read M, Waring W. International standards for neurological classification of spinal cord injury (revised 2011). J Spinal Cord Med 2011;34:535–546.
Lindberg F, Ohberg F, Brodin LA, Gronlund C. Assessment of intramuscular activation patterns using ultrasound m-mode strain. J Electromyogr Kinesiol 2013;23:879–885.
Maganaris CN, Baltzopoulos V, Sargeant AJ. Human calf muscle responses during repeated isometric plantarflexions. J Biomech 2006;39:1249–1255.
Mayans D, Cartwright MS, Walker FO. Neuromuscular ultrasonography: Quantifying muscle and nerve measurements. Phys Med Rehabil Clin North Am 2012;23:133–148.
Nakanishi N, Tsutsumi R, Okayama Y, Takashima T, Ueno Y, Itagaki T, Tsutsumi Y, Sakaue H, Oto J. Monitoring of muscle mass in critically ill patients: Comparison of ultrasound and two bioelectrical impedance analysis devices. J Intensive Care 2019;7:61.
Narici MV, Binzoni T, Hiltbrand E, Fasel J, Terrier F, Cerretelli P. In vivo human gastrocnemius architecture with changing joint angle at rest and during graded isometric contraction. J Physiol 1996;496:287–297.
Pierotti DJ, Roy RR, Bodine-Fowler SC, Hodgson JA, Edgerton VR. Mechanical and morphological properties of chronically inactive cat tibialis anterior motor units. J Physiol 1991;444:175–192.
Pillen S, Verrips A, van Alfen N, Arts IM, Sie LT, Zwarts MJ. Quantitative skeletal muscle ultrasound: Diagnostic value in childhood neuromuscular disease. Neuromuscul Disord 2007;17:509–516.
Pillen S, Arts IM, Zwarts MJ. Muscle ultrasound in neuromuscular disorders. Muscle Nerve 2008;37:679–693.

Reeves ND, Narici MV. Behavior of human muscle fascicles during shortening and lengthening contractions in vivo. J Appl Physiol 2003;95:1090–1096.

Sawilowsky S, Sawilowsky J, Grissom RJ. Effect size. Berlin/Heidelberg: Springer; 2011. p. 426–429.

Shi J, Zheng YP, Chen X, Huang QH. Assessment of muscle fatigue using sonomyography: Muscle thickness change detected from ultrasound images. Med Eng Phys 2007;29:472–479.

Silva NA, Sousa N, Reis RL, Salgado AJ. From basics to clinical: A comprehensive review on spinal cord injury. Prog Neurobiol 2014;114:25–57.

Whittaker JL, Teyhen DS, Elliot JM, Langevin KCHM, Dahl HH. Rehabilitative ultrasound imaging: Understanding the technology and its applications. J Orthop Sports Phys Ther 2007; 37:434–449.